Progress In Electromagnetics Research C, Vol. 110, 253–265, 2021

A New Fast, Memory Efficient Wireless Electromagnetic Beamformer Antenna with Fast Tracking for 5/6G Systems

Herman Kunsei[1, *], Kandasamy Pirapaharan[2], and Paul R. P. Hoole[1, 3]

Abstract—The much-anticipated year of 5G deployment has lapsed, and yet much research is ongoing on the 5G New Radio (NR) interface. The quality of service and user experience is dependent on a stable and signal strength of the wireless communication link. To serve multiple users per sector accessing dedicated and unique services pose a challenge for passive antenna systems with omnidirectional beams. Smart 5G antenna technology with null forming and beamforming promises to serve mobile users well by offering a reliable wireless communication link. To address this need, we propose a 2×2 MIMO antenna capable of electronically forming electromagnetic beams in one direction and nullifying electromagnetic beams in any undesired direction. We demonstrate the usefulness of the proposed antenna by evaluating five cases that showed interesting insights, confirming the hypothesis that it is possible to implement beamforming in a 2×2 MIMO system with less computing power and minimum number crunching. What is novel and attractive about the proposed antenna are: (a) forming a beam with maximum directivity towards the desired user, while (b) simultaneously producing nulls towards an undesirable transmitter, and (c) a fast electromagnetic tracking module inbuilt into it so that the base station antenna may constantly track and maintain the communication link with the moving wireless transceiver or cell phone. While most wireless mobile systems use two separate software modules for beamforming and tracking the mobile station, the method presented here does electronic beamforming and tracking of the mobile user with a single low memory, computationally fast technique within the range of 10 ms to 19 s.

1. INTRODUCTION

The pure 5th Generation (5G) New Radio (NR) interface must be smart enough to handle massive user traffic with different needs at high speeds, low latency, and greater reliability. These are the requirements which dictate that new smart antennas developed for the 5G network must satisfy. The smart antenna must be able to form an accurate and stable electromagnetic radiation pattern to the desired user with improved spectrum efficiency at high speeds [1–3]. The need for greater reliability can be implemented using massive multiple input and multiple output (MIMO) active antenna systems [2, 4].

Current research has been conducted on MIMO antenna systems for 5G networks. While more antenna elements offer very accurate beam forming performance, it also comes at the cost of high computational needs and mechanical complexity [5, 6]. Therefore, the research of 2×2 MIMO antenna systems for 5G or 6G application is a valuable research area [7–10]. [7] proposes a 2×2 MIMO array that covers the 5G range of frequencies with fixed beams. A tri-band 2×2 MIMO antenna is presented in [8] that offers a compact antenna, suitable for mobile devices, operating at 28, 38, and 60 GHz. A reconfigurable antenna presented in [9] offers five stable switched beams at 28 GHz based on a slot antenna design. However, the implementation of slot antennas is mechanical and bulky which is not

Received 18 September 2020, Accepted 25 February 2021, Scheduled 10 March 2021

* Corresponding author: Herman Kunsei (herman.kunsei@pnguot.ac.pg).

[1] Department of Electrical and Communications Engineering, University of Technology, Papua New Guinea. [2] Faculty of Engineering, University of Jaffna, Jaffna, Sri Lanka. [3] Wessex Institute of Technology, Southampton, United Kingdom.

applicable in mobile devices. In [10], the authors present a 2×2 MIMO slotted antenna for 4G and 5G applications. The compact antenna is sufficient to fit in mobile devices. However, selecting from a set of fixed beams would be less effective for high mobility devices. A 4×4 MIMO antenna in [11] offers a wider bandwidth and acceptable gain; however, the switch fixed beams limit the applications of this antenna system for 5G or 6G applications.

In recent developments, the limited 5G adapted networks have highlighted some new insights, which are classified as the next 6th generation of mobile networks, 6G. While 5G promised wider coverage on land, 6G networks would provide coverage on land as well under water, over water, and in space [12]. New user cases and reliability requirements have made the uplink as important as the downlink [12, 13]. This requirement implies that the downlink and uplink data rates in 6G network would be more symmetrical. A more practicable approach is to use steerable antenna [13] to implement the symmetrical link.

Therefore, we present a 2×2 MIMO electromagnetic model of a beam steering antenna and demonstrate some features that make the proposed antenna a fast, memory efficient wireless antenna with fast tracking that is useful for 5G and 6G applications [14–16].

2. PROPOSED 2×2 MIMO ANTENNA

MIMO antenna systems utilize the angle of arrival (AoA) of a signal to determine the angle of departure (AoD) to transmit beam or null discreetly [16]. Fig. 1 shows a simplified transceiver antenna with two elements of the proposed MIMO antenna system. The reference transceiver antenna is also a two-element antenna. However, the focus is on beamforming of the two-element receiver array, which is based on the AoA and beamforming code being applied. A complete analysis of the model would include additional transmitting set of weights, w_3 and w_4 with different receiving angles, θ_2. However, based on the principle of reciprocity in Antenna Theory [17], the analysis of the complete 2×2 MIMO antenna system is equivalent to a scaled version of a transceiver in receiving antenna mode. To counter the effects of channel distortion, some preprocessing is assumed at the transmitting antennas before transmission as described in [18] where the data stream is precoded. Thus, the two received signals are enough to convey the four-variable input to the complete 2×2 MIMO antenna system with independent beamforming done at both two-element antennas shown in Fig. 1.

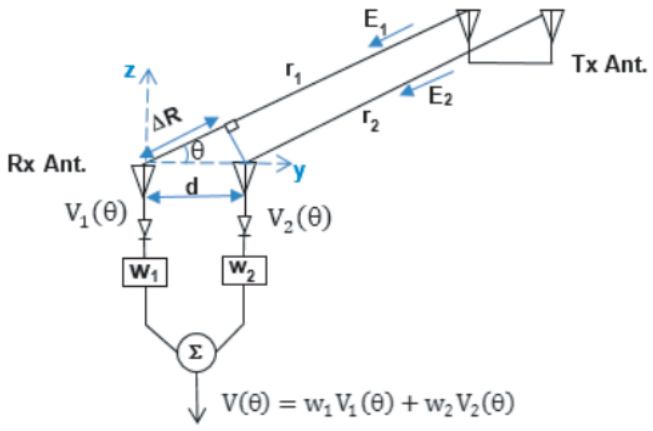

Figure 1. 2×2 precoded MIMO smart antenna.

The reduced number of input variables for processing offers an underlying advantage of the proposed antenna system — fast processing. The complete MIMO systems would require the processing of four input variables. However, as shown below, the proposed system only requires two input-variables to steer the beam and create nulls in the desired direction. Thus, we anticipate that the processing of two antenna elements on each of the two transceivers would be much faster and require less computation

power in the hardware implementation [5, 6]. The operational procedure of the model will be discussed next.

The orientation of the antenna is normal to the incident plane of the far-field electromagnetic signals originating from the transmitting antenna if the transmitting and receiving antennas are at the same height. That may not be the case in every setup as shown in Fig. 1. Thus, two uniform plane waves arrive at the receiver antennas with electric fields, E_1 and E_2, with known magnitude and unknown phase having travelled a distance r_1 and r_2, respectively. The distances r_1 and r_2 are unknown but are not necessary for beamforming. However, the difference between r_1 and r_2 is determined from the AoA, θ, of the waves which is measured from the horizontal axis of the antenna. This difference is given as

$$\Delta R = r_1 - r_2 = r_1 - d\cos\theta \tag{1}$$

where d is the separation distance between the elements, ΔR the difference between r_1 and r_2, r_1 the distance travelled by E_1, and r_2 the distance travelled by E_2. Once θ is determined, r_2 can be calculated with d, which is measured in wavelengths, λ. The beamforming code developed below based on this model is frequency and medium dependent. The selection of the specific center frequency of the 5G communication band can be from either the FR1 or FR2 band. The stability of the beamforming code when the frequency of operation shifts from center frequency is investigated in this paper. In this paper, we use the minimum separation distance of $\lambda/2$ with a center frequency of 60 GHz.

The electric fields, E_1 and E_2, induces voltages into the vertical antenna elements to become voltages $V_1(\theta)$ and $V_2(\theta)$, respectively. The output of the antenna array is the sum of the individual branch signal being multiplied by the respective weights $w_1(\theta)$ and $w_2(\theta)$. Thus, the output, or total received signal, is defined as:

$$V(\theta) = w_1 V_1(\theta) + w_2 V_2(\theta) \tag{2}$$

From Eq. (2), we note that the AoA can be the desired angle for maximum direction or null in the direction of the interferer. Therefore, the smart antenna challenge we are addressing may be defined in five cases. Case 1 involves how to null the total received signal from an interfering transmitting source by making $V(\theta) = 0$. That is, when the interfering source is at $\theta = \theta_i$, the output must be zero, $V(\theta_i) = 0$. Case 2 concerns maximizing the beam in the direction of the received signal from the desired transmitting source. We call this AoA as $\theta = \theta_{\max}$, thus in that direction the voltage is maximum, $V(\theta_{\max}) = V_{\max}$. Case 3 is not useful as discussed in Section 3.2. Case 4 explores the challenge of implementing cases 1 and 2 simultaneously, i.e., how to simultaneously produce a maximally directed beam towards the desired source signal at $\theta = \theta_{\max}$ and to produce a null in the direction of the undesired interfering source at $\theta = \theta_i$. Finally, extending case 2 we consider the challenge of tracking the desired user. Once the position of the desired user is known, we use case 2 to form a new beam with maximum directivity in the new direction of the desire user. While in cases 1, 2, and 4 we assume that the location of the desired transmitting source and the interferer are known, in case 5 the location is unknown, thus we track the mobile transmitter, by determining a new AoA, $\theta_{\max}$. In general, a separate mobile station tracking algorithm is used to determine the position of the mobile station as it moves within the cell of each base station and from one cell to another cell [19]. In terms of the AoA, it is a known variable.

The weights in Eq. (2), w_1 and w_2, are the unknown variables to be determined in each of the cases, case 1 to case 5, such that the desired results are obtained. Section 3 discusses the conditions and results for each case. The weights are determined using numerical method in MATLAB. The beamforming codes developed for each of the mathematical models are presented in the next section.

3. SIMULATION SETUP

3.1. Case 1 Nullifying an Interferer $V(\theta) = 0$, $AF = 0$

The objective of case 1 is to produce a null in the direction of an interferer. Thus from Eq. (2), we let $w_1(\theta) = 1$ and $w_2(\theta) = e^{(\pm j\delta)}$ where the phase, δ, is unknown. The AoD for the null to the interferer is $\theta = \theta_i$, and we need to find the phase angle, δ. Since $w_1(\theta) = 1$, then Eq. (2) is simplified to:

$$V(\theta) = V_1(\theta) + w_2 V_2(\theta) \tag{3}$$

$$where\ V_1(\theta) = V(\theta)e^{(-jkr_1)}\ and\ V_2(\theta) = V(\theta)e^{(-jkr_2)} \tag{4}$$

Therefore, substituting Eq. (4) in Eq. (3) and inserting Eq. (1) into Eq. (3) becomes

$$V(\theta) = V(\theta)e^{(-jkr_1)}\left(1 + e^{j(kd\cos\theta-\delta)}\right) \tag{5}$$

Thus, the array factor,

$$AF = 1 + e^{j(kd\cos\theta-\delta)}. \tag{6}$$

If we let $kd\cos\theta - \delta = \beta$, then Eq. (6) is simplified to $1 + e^{j\beta}$. This implies that for Eq. (6) to be zero, $e^{j\beta} = -1$, that is, $\beta = \pm\pi$, because the induced voltage would be zero, $V(\theta) = 0$. For clarity, the phase must be that of the interferer, labeled as $\delta = \delta_i$, and the AoA must be that of the interferer, $\theta = \theta_i$.

In other words, $e^{j(kd\cos\theta_i-\delta_i)} = -1$ will ensure that AF $= |1 - 1| = 0$. We let $kd\cos\theta_i - \delta_i = \beta$, then substitute it in Eq. (6) to give $e^{(-jk\beta)} = -1$ where $kd\cos\theta_i - \delta_i = \pm\pi$. Therefore, the phase angle that will produce a null to the interferer is $\delta_i = kd\cos\theta_i - \pi$. Hence, the array factor is

$$\begin{aligned}
\text{AF} &= \left|1 + e^{(-j(kd\cos\theta-\delta_i))}\right| \\
&= \left|1 + e^{(-j(kd\cos\theta-kd\cos\theta_i+\pi))}\right| \\
&= \left|1 + e^{(-j\pi)}e^{(-j(kd\cos\theta-kd\cos\theta_i))}\right|, \text{ since } e^{(-j\pi)} = -1. \\
&= \left|1 - e^{(-j(kds\cos\theta-kd\cos\theta_i))}\right| \\
&= \left|1 - e^{(-jkd(\cos\theta\cos\theta_i))}\right| \\
&= \left|1 - e^{(-j\gamma)}\right| \text{ where } \gamma = kd(\cos\theta\cos\theta_i) \\
&= \left|e^{(-j\gamma/2)}\left(e^{(j\gamma/2)} - e^{(-j\gamma/2)}\right)\right| \\
&= \left|e^{(-j\gamma/2)}2\sin(\gamma/2)\right| \text{ since } 2\sin\alpha = (e^{j\alpha} - e^{-j\alpha}) \\
&= 2\sin(\gamma/2) \text{ since } e^{(-j\gamma/2)} \text{ only affects phase and not magnitude of the signal.}
\end{aligned} \tag{7}$$

The generalized array factor is

$$AFN = \text{AF}/2 = \sin(\gamma/2) \tag{8}$$

$$where\ \gamma = kd(\cos\theta\cos\theta_i) \tag{9}$$

3.2. Case 2 Maximum Directivity to Desired User, $V(\theta_{\max}) = 1$, $AF = 2$

The objective of case 2 is to form the beam of maximum directivity toward the desired user. This is achieved by making the second term in Eq. (6) to be 1, as in:

$$e^{j(kd\cos\theta-\delta)} = +1 \tag{10}$$

Then AF $= 1 + e^{j(kd\cos\theta-\delta)} = 1 + 1 = 2$, which is when the radiation pattern is at maximum. Let

$$kd\cos\theta - \delta = \beta \tag{11}$$

For Eq. (10) to be positive 1, $e^{j\beta} = +1$, Eq. (11) must be evaluated as $kd\cos\theta - \delta = 0$. Now the phase angle must be the phase of the desired user, thus $kd\cos\theta - \delta = 0$ becomes $kd\cos\theta - \delta_m = 0$. The phase angle for maximum directivity is defined as:

$$\delta_m = kd\cos\theta_m \tag{12}$$

Substituting Eq. (12) into Eq. (6) gives the array factor in case 2 as:

$$\text{AF} = \left|1 + e^{j(kd\cos\theta-\delta_m)}\right| = \left|1 + e^{j(kd\cos\theta-kd\cos\theta_m)}\right| \tag{13}$$

Let $\gamma = kd(\cos\theta - \cos\theta_m)$, then Eq. (13) is reduced to

$$\text{AF} = \left|1 + e^{(-j\gamma)}\right| = 2\cos(\gamma/2) \tag{14}$$

3.3. Case 3 Both Phase Shift Angles Delta Are Not Zero, $\delta_1 \neq 0$. Both Weights Have a Magnitude Which Is 1

Considering Fig. 1, the output signal is:

$$\begin{aligned} V &= w_1 V_1(\theta) + w_2 V_2(\theta) \\ &= w_1 V_0 e^{(-jkr_1)} + w_2 V_0 e^{(-jkr_2)} \\ &= w_1 V_0 e^{(-jkr_1)} + w_2 V_0 e^{(-jk(r_1 - d\cos\delta\theta))} \\ &= w_1 V_0 e^{(-jkr_1)} + w_2 V_0 e^{(-jkr_1)} e^{(jkd\cos\theta)} \\ &= V_0 e^{(-jkr_1)} \left(w_1 + w_2 e^{(jkd\cos\theta)}\right) \end{aligned}$$

The array factor is

$$\begin{aligned} \mathrm{AF} &= w_1 + w_2 e^{(jkdcos\theta)} \\ &= e^{(j\delta_1)} + e^{(j\delta_2)} e^{(jkdcos\theta)} \text{ where } w_1 = e^{(j\delta_1)} \ \& \ w_2 = e^{(j\delta_2)} \\ &= e^{(j\delta_1)} \left(1 + e^{(j\delta_2 - \delta_1)} e^{(jkd\cos\theta)}\right) \\ &= e^{(j\delta_1)} \left(1 + e^{j\delta} e^{(jkd\cos\theta)}\right) \text{ where } \delta = \delta_2 - \delta_1 \\ &= e^{(j\delta_1)} \left(1 + e^{(jkd\cos\theta + \delta)}\right) \end{aligned} \tag{15}$$

Notice from Eq. (15) that if $\delta_1 = 0$, then the relationship is reduced to either case 1 or case 2. Thus, case 3 is not a useful case.

3.4. Case 4 Simultaneous Varying of Delta and Weight

Another challenging scenario is case 4 where the weights and phase are varied simultaneously to form the beam towards a desired user while simultaneously forming a null towards an interferer. As shown in Fig. 1, the two signals arriving at either antenna element would have two different phases, δ_1 and δ_2, due to the different distances travelled. The phase defines the weight being applied by the respective signal processing branch of the antenna system as shown in Fig. 1. The objective of the smart antenna remains the same, to form the beam with maximum directivity towards the desired user and a null towards an interferer.

The output signal is then:

$$\begin{aligned} V &= V_1(\theta) + V_2(\theta) \\ &= w_1 V_1(\theta) + w_2 V_2(\theta) \\ &= w_1 V_0 e^{(-jkr_1)} + w_2 V_0 e^{(-jkr_2)} \end{aligned} \tag{16}$$

since $r_2 = r_1 - \Delta R = r_1 - d\cos\theta$, (16) is expanded to

$$w_1 e^{(j\delta_1)} V_0 e^{(-jkr_1)} + w_2 e^{(j\delta_2)} V_0 e^{\left(-jk\left(r_1^{d\cos\theta}\right)\right)} \tag{17}$$

Assume that the first phase angle shift is zero, $\overset{\delta}{1} = 0$, and the amplitude of the second weight, w_2, is 1, then Eq. (17) is reduced to

$$\begin{aligned} &= w_1 V_0 e^{(-jkr_1)} + e^{(j\delta_2)} V_0 e^{(-jkr_1)} e^{(jkd\cos\theta)} \\ &= V_0 e^{(-jkr_1)} \left(w_1 + e^{(j\delta_2)} e^{(jkd\cos\theta)}\right) \end{aligned} \tag{18}$$

The array factor for case 4 is then:

$$\mathrm{AF} = w_1 + e^{(j(kd\cos(\theta + \delta_2))} \tag{19}$$

The normalized array factor is then:

$$\mathrm{AF}_N = \mathrm{AF}/2 = 1/2 \left| w_1 + e^{(jkd\cos\theta + \delta_2)} \right| \tag{20}$$

The AoD in Eq. (20) can either be that of the desired user, θ_m, or an interferer, θ_i. To produce a null in θ_I, the normalized antenna array factor must be zero, $\mathrm{AF}_N = \mathrm{AF}/2 = 0$. To produce a maximum directed beam in θ_m, the normalized antenna array factor must be one, $\mathrm{AF}_N = \mathrm{AF}/2 = 1$. Using the alternate form of Eq. (20), we have

$$\mathrm{AF}_N = 1/2\,|w_1 + \cos(kd\cos(\theta + \delta_2)) + j\sin(kd\cos(\theta + \delta_2))| \tag{21}$$

Notice from Eq. (21) that there are two unknowns, w_1 and δ_2. To solve for w_1 we equate $\mathrm{AF}_N = 0$ and solve for w_1:

$$\begin{aligned} &1/2|w_1 + \cos(kd\cos(\theta_i + \delta_2)) + j\sin(kd\cos(\theta_i + \delta_2))| = 0 \\ &w_1 + \cos(kd\cos(\theta_i + \delta_2) + j\sin(kd\cos(\theta_i + \delta_2)) = 0 \\ &w_1 = -\cos(kd\cos(\theta_i + \delta_2)) - j\sin(kd\cos(\theta_i + \delta_2)) \end{aligned} \tag{22}$$

We then use the condition for maximum directivity, $\mathrm{AF}_N = 1$, to solve for the phase, δ_2:

$$1/2\,|w_1 + \cos\left(kd\cos\left(\theta_m + \delta_2\right)\right) + j\sin\left(kd\cos\left(\theta_m + \delta_2\right)\right)| = 1 \tag{23}$$

Since solving for the analytical solution would be a mammoth task, Equations (22) and (23) were solved symbolically in MATLAB^{TM}.

3.5. Case 5 Tracking a Mobile Station

In case 5, we present a simple analytical method to track a mobile station (MS) with a two-element smart array antenna arrangement presented above. The mobile transmitter or MS may move in the forward or reverse direction. In this case, we only consider the forward direction. The reverse direction can be analyzed by negating the angles.

We begin with Eq. (8) where at the initial position of the MS, the normalized AF is 1, i.e., maximum, at point A in Fig. 2 with the phase angle at θ_m which maximizes the electromagnetic radiating beam towards point A. The normalized antenna factor for case 5 is shown in Eq. (24).

$$AF_N = \cos(\gamma/2) = 1 \text{ where } \gamma = kd\,(\cos\theta + \cos\theta_m) \tag{24}$$

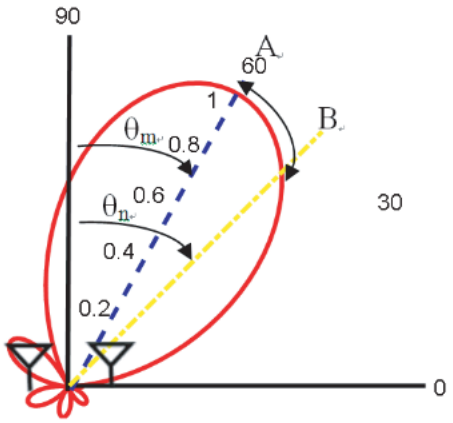

Figure 2. Case 5 movement in the same circular away from the main beam. Considering movement from A to B as positive and the opposite direction as negative.

At the new position, B, the nominalized antenna array factor is some value, p (with $p < 1$), and the new angle is θ_n. From Eq. (24) the angle is defined as $\gamma = kd(\cos\theta_n + \cos\theta_m)$ where θ_n is the new AoD for maximum directivity. Thus, the new angle can be calculated from power level at that point:

$$p = \cos(kd(\cos\theta - \cos\theta_m)/2) \tag{25}$$

Rearranging Eq. (25) for the new desired angle θ_n yields

$$\theta_n = \cos^{-1}\left[\left(2 * \cos^1(p)\right) / \left(kd + \cos\theta_m\right)\right] \tag{26}$$

Using the new angle, we determine the location of the MS as the first step. In the second step, the new angle becomes the AoD where a new maximum directivity beam is formed towards the MS. The new angle in $\gamma = kd(\cos\theta - \cos\theta_m)$ is used to determine the new phase angle δ of the smart antenna phase shifter and form the new beam in the new direction. The two-step process allows us to both track the MS and form the beam with maximum directivity towards the new position of the moving MS.

4. SIMULATION RESULTS

Simulation results of cases 1, 2, 4, and 5 are shown in Figs. 3 to 6, respectively. Since case 3 is similar to either case 1 or 3, it is not mentioned in this section. Fig. 3 shows case 1 results where nulls are formed in the 30°, 45°, 90°, 120°, 270°, and 345° directions. To aid visibility, black arrows are drawn to indicate the angles at which the interfering source is present. It can be observed that the model is in good agreement with theory, giving zero reception power level in the direction of the interferer.

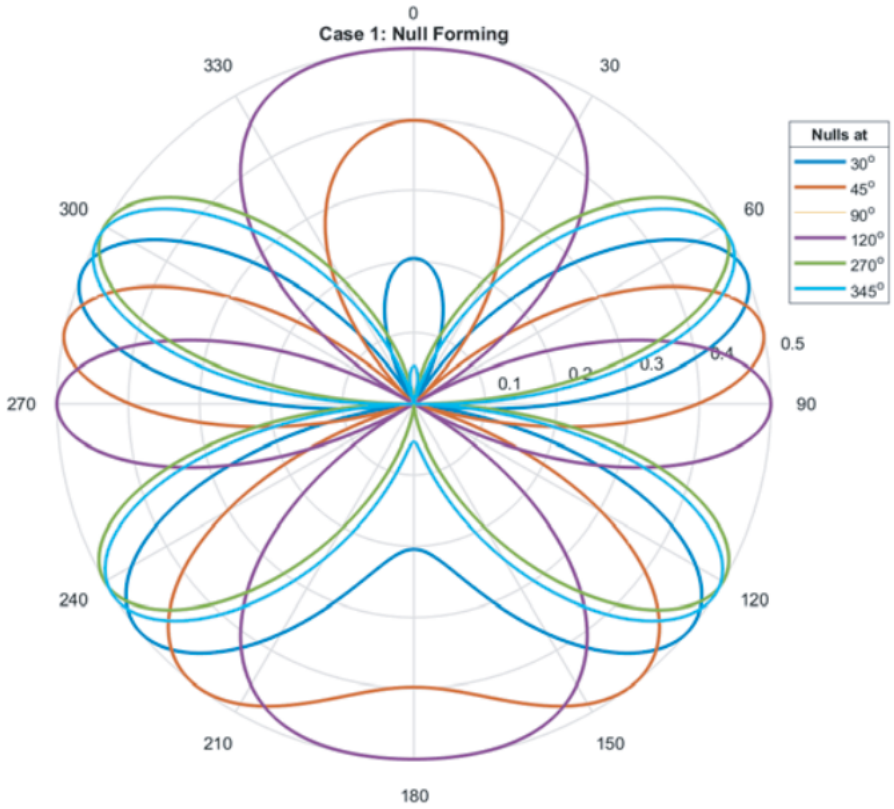

Figure 3. Case 1 forming of null in the direction of the interferer.

Case 2 results are shown in Fig. 4 where the maximum directivity of the beam should be formed in the 30°, 45°, 90°, 120°, 270°, and 345° directions. It can be observed that the analytically derived beamforming code output is in good agreement with the desired direction for maximum directivity (i.e., maximum array factor of the beam).

Figure 5 shows the beams formed to verify case 4 where θ_m (position of desired MS) and θ_i (position of the interfering MS) are taken to be 30° and 300°; 120° and 30°; 180° and 300°; and 340° and 270° for the blue, red, yellow, and purple plots, respectively. The nulls are clearly seen in Fig. 5, which are similar to the plots in Fig. 3 and are in good agreement with the specifications. The beamforming in desired maximum directivity shows some good agreement when the θ_m and θ_i angle pairs are 90° and 0°, 120° and 60°, and 150° and 75°, respectively, while the worst case is the pair 60° and 35°. It appears that the beamforming code offers a higher resolution when the difference between θ_m and θ_i is more than 60°. The worst case difference between θ_m and θ_i is 25°, while the differences for the acceptably

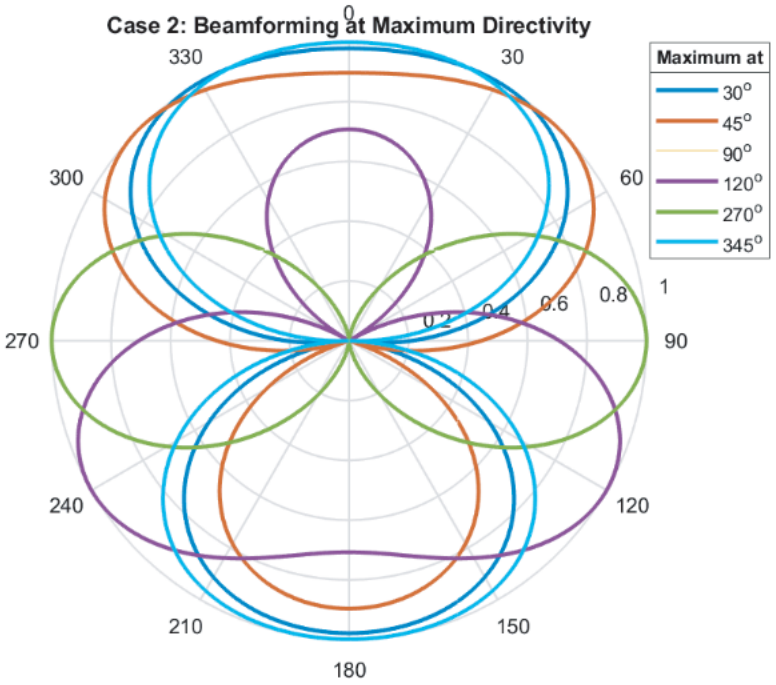

Figure 4. Case 2 forming of a beam with maximum directivity in the desired direction.

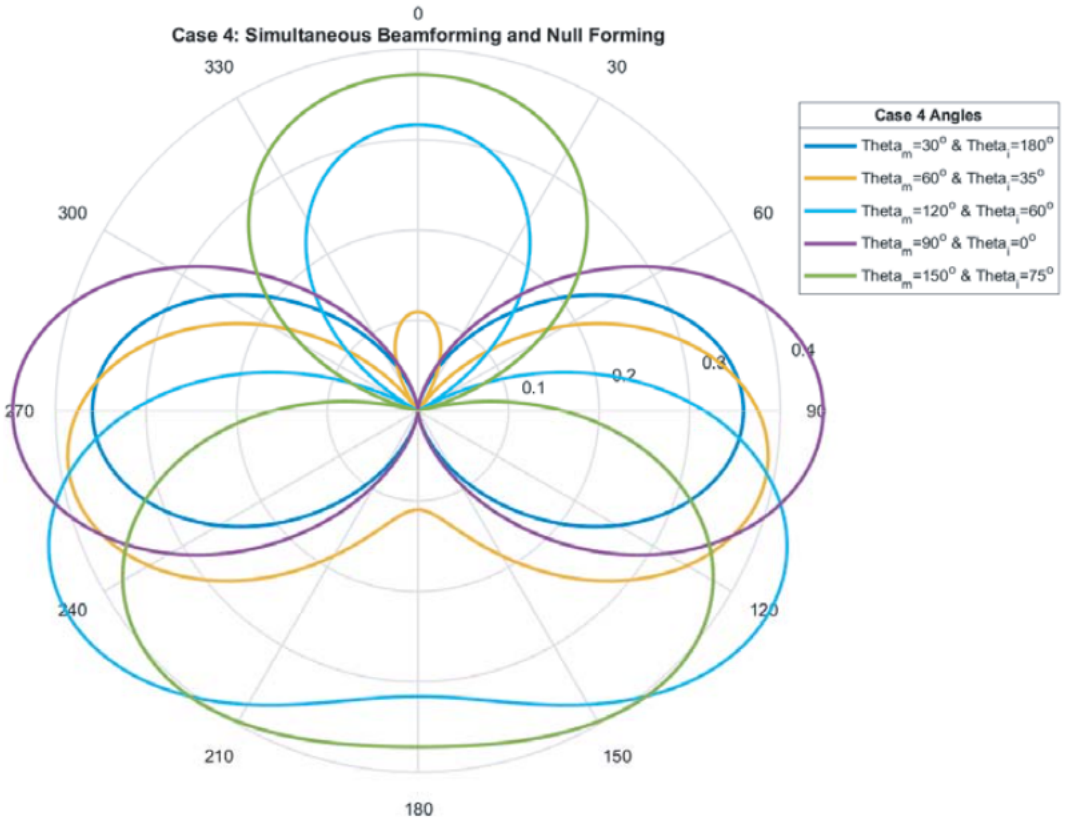

Figure 5. Case 4 simultaneous beam and null forming for five angles.

accurate cases are 90°, 60°, and 75°. Thus, when the difference between θ_m and θ_i is more than 60°, the beamforming code can form an acceptable maximum beam and null. When the difference between the angle pairs is less than 60°, the beamforming code fails to form a distinctive beam with maximum directivity.

In Fig. 6, we see seven plots showing the tracking of the moving MS as evident by new plots as the power level decreases due to movement in the positive direction. The beamforming code shows agreeing results of the concept of electromagnetically tracking the MS and beamforming using the same code. This technique promises to be a simple, fast, and power efficient method of tracking mobile users. To validate the speed of the code, the execution time was measured.

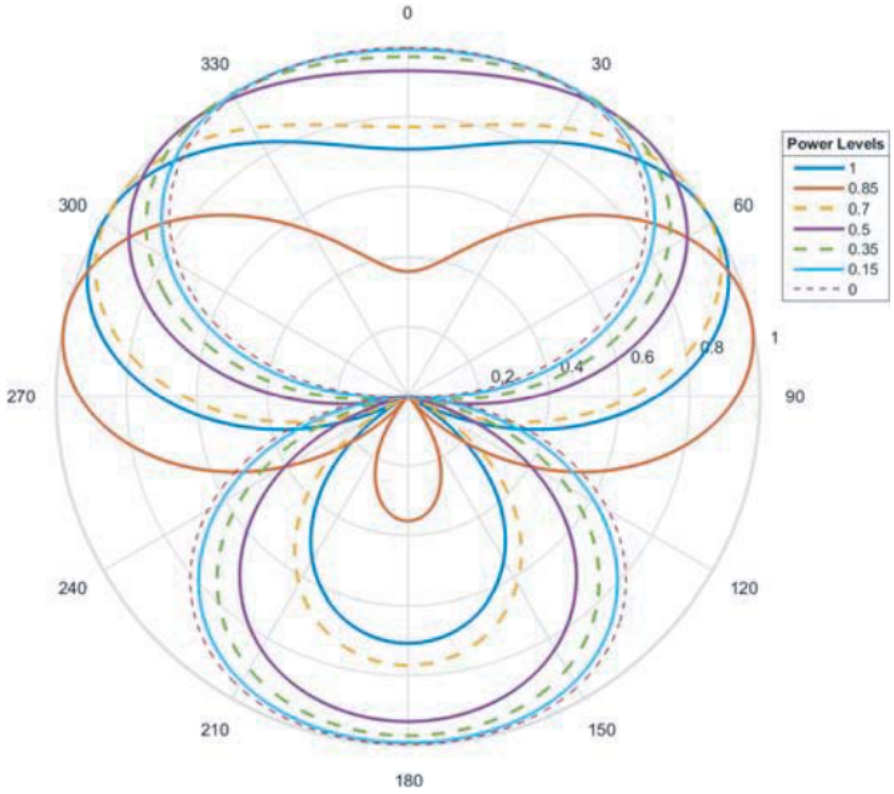

Figure 6. Case 5 tracking of mobile user position and beamforming in the new direction.

The time taken to generate and calculate the weights for beamforming or null forming in the desired direction varies from case to case. On average, the beamforming code took 335.9 ms to form a null (case 1) and 175.1 ms to maximize (case 2) the beam in the desired direction from sixteen AoA, trialed twice giving a sample size of thirty-two readings. For case 4, the beamforming code took an average of 19.32 seconds to form the null and the maximum beam from a total of twenty-two readings. While in evaluating the speed of case 5, four different desired angles were used to determine an average speed of the beamforming code. It was observed that for maximum power level, which is array factor of 1, it took an average of 76.27 ms to determine the direction and form the beam. As the MS moves away from the maximum directivity of the beam, AF = 1, the power level decreases. The average time to determine the next subsequent AoA and beamforming is less than 10 ms as shown in Table 1.

Table 1. Beamforming code convergence time for Case 5.

Array Factor	1	0.85	0.7	0.5	0.35	0.15	0
Time (ms)	76.27	8.486	7.65	6.519	11.012	2.748	2.603

5. DISCUSSION

5.1. Beamforming Code Application

The beamforming code was applied in four cases. Fig. 3 shows the simulation results for case 1, where a null is formed by the antenna array to cancel the signal from an interfering source. For clarity, black arrows point to the nulls for each angle in Fig. 3. On the other hand, Fig. 4 shows the scenario where the antenna array would form a beam in the desired direction of an MS with which the two-element smart antenna transceiver needs to maintain maximum reception and transmission. The desired MS should be kept in the direction of maximum directivity. In both cases, there is good agreement for six angles of nulls and maximum directivity. The maximum angle is where the plot crosses the outer signal power of 1. The results are comparable to that presented in [9].

The best results for case 4 are shown in Fig. 5 with five angles of maximum directivity and nulls for the 2×2 MIMO system. More elements would be needed to form a perfect beam. However, the first set of angles show 100% agreement in the null at 35° and half power in the desired maximum direction of 60°. The second set also shows 100% agreement in the null and much better beam in the maximum direction. The third set of angles show 100% agreement in forming the null at 120° and 100% agreement in the maximum direction with the main lobe despite the lower power. The other two sets all show similar performances. It is evident that the 2×2 MIMO antenna can form a null and beam in the desired direction. However, forming a much efficient beam would require more antenna elements [20] with a nonlinear array [21].

Case 5 results are shown in Fig. 6. As defined in Eq. (26), the reduced power level indicates the angular distance of movement from previous maximum power level. The initial position is the AoA with array factor of 1 which can be the direction of maximum directivity. As the MS moves, the power level should decrease. The change in power level defines the resolution of the tracking and is used to determine the new AoD for beamforming. Thus, if the next reception power level is 0.7, the tracking algorithm accurately locates the new MS position to be at 30°. The direction of movement can either be clockwise or anticlockwise as defined by movement of the MS, as shown in Fig. 2. The alternate implementation of this case is the method outlined in [22], where phase array antennas were used in tracking and beamforming, which can be less power efficient. Employing artificial intelligence (AI) may improve the performance of the antenna [12, 23]. The incorporation of AI in this work will be further investigated as an extension of this work to introduce both AI driven antennas [24] and analytically (angle shift) driven single beam antennas [20] in the context of specific applications [15, 16]. This is a valuable research area in which more work is needed to improve the application-dependent usefulness of smart beamforming antennas [3]. The advantages of our proposed beamforming code are that it is simpler and requires less computational power and fast.

5.2. Speed of Processing of the Beamforming Code

In addition, the proposed beamforming code is fast. The speed of the beamforming code to converge is as low as 10 ms to 19 s. It is anticipated that cases 1 and 2 should offer shorter processing time than cases 4 and 5 because of the number of unknown variables involved. It was case 4 that took the longest processing time of 19 s. The fast time of 10 ms was to move the beam between different power levels in case of movement of the MS considered in case 5. Despite that, the first step took longer to track and form the first beam, and the subsequent steps took a fraction of time taken for the first step to generate the new beam. The evaluation of this beamforming code in hardware is a valuable contribution to the development of smart antennas as discussed in [3] where accurate and stable beamforming algorithm is needed to add value to massive MIMO antennas for 5G and 6G mobile networks. The technique presented here may be readily extended to massive MIMO systems.

5.3. Stability of the Beamforming Code

Finally, an in-depth study of the accuracy of the proposed beamforming code will be a follow-up work to this paper. However, we show the stability of the beamforming code in Fig. 7 by generating the five beams for case 5 at three different operating frequencies in the 5G FR1 and FR2 bands. Note that

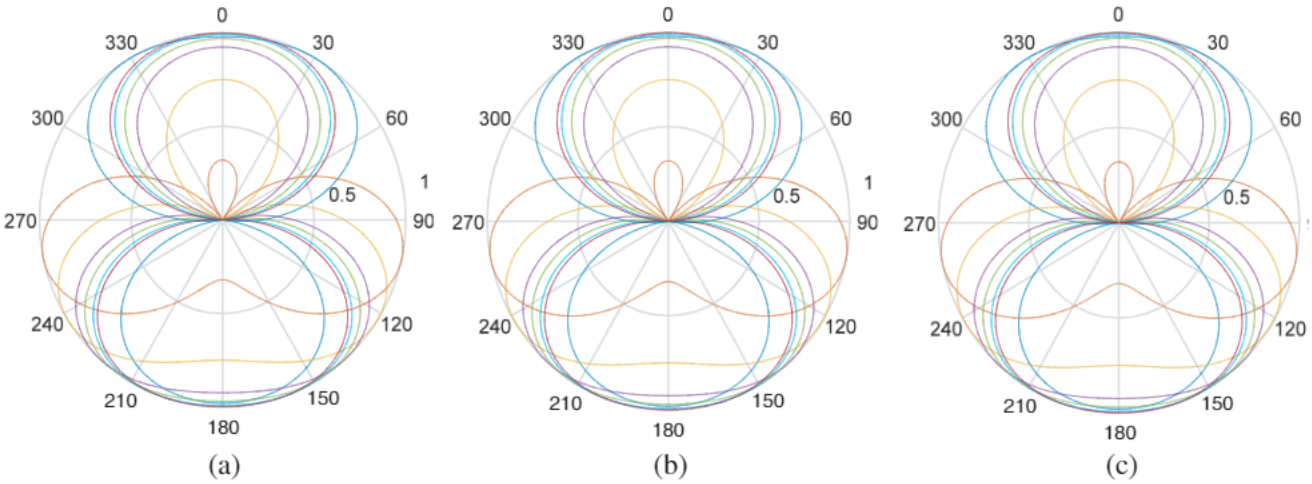

Figure 7. Stability plots for Case 5 for three different frequencies; (a) 6 GHz, (b) 30 GHz and (c) 60 GHz with AoA of 240° as the prescribed $\theta_{\max}$.

there is not much difference between the beams formed as the frequency changes. We have shown that the proposed beamforming code is functional and stable. It is anticipated that by employing artificial neural network (ANN) algorithm to determine the weights for the movement of the mobile stations, the beamforming code will be effective in high multipath environments [3].

6. CONCLUSION

A fast, memory efficient beamforming antenna with mobile station tracking was presented in this paper. The efficiency of the proposed 2×2 MIMO was investigated by deriving the normalized array factor for four cases that illustrated the benefits of smart beamforming antennas presented in this paper. These benefits are dealing with interferers, reaching the desired user with optimum signal strength, simultaneously blocking interference and connecting legitimate users. Finally, a fast and accurate tracking of the MS in two dimensions was an added feature of the work presented. The beamforming code derived from the antenna array factor showed acceptable results when separately producing nulls and maximum beams. Some challenges exist when producing nulls and maximum beams simultaneously. These challenges include the accuracy and stability of producing the maximum beam. These challenges will be the focus of the next phase of this research work.

The benefit of model-based tracking of the MS and maintaining a reliable link showed promising results. While the shape of the beam changes as the MS moves to new positions, the tracking and beamforming function of the code is straight forward and converges faster in operation. The inherited nature of the beam pattern at each new position offers the variable to determine the location of the MS, and the new beam helps establish a good link with the user within the coverage area in two dimensions, or the x-y plane. Tracking should continue to extend the coverage area thus minimizing handoff. More research is required to confirm the rate and range of coverage area before handoff to another cell, as well as extending the tracker to three-dimensional scenarios.

The processing speed of the beamforming code is promising with the fastest processing time of 10 ms for tracking an MS while the slowest processing time of 19 s for simultaneous null and maximum beamforming function. Evaluating the performance of beamforming code on a standard computer implies that on a dedicated controller, the processing time would be much shorter. Future work will include the verification of the beamforming code on custom designed hardware with the aid of embedded ANN to effectively perform multiple tasks using little memory and shorter processing time.

REFERENCES

1. *IMT Vision — Framework and Overall Objectives of the Future Development of IMT for 2020 and beyond*, 2015.
2. Morley, D., "5G small cells and cable: Realizing the opportunity," Shaw Communications Inc/Freedom Mobile, Alberta, Technical Report October 2018, 2018.
3. Al, E., M. Ismail, R. Nordin, and N. F. Abdulah, "Beamforming techniques for massive MIMO systems in 5G: Overview, classification, and trends for future research," *Frontiers of Information Technology & Electronic Engineering*, Vol. 18, 753–772, 2017.
4. Anritsu, "Ten 5G Challenges for Engineers to Overcome," 8, ed.: Anritsu, 2018.
5. Joseph, M., O. Tobi, and G. A. Igwue, "Development of a new adaptive beam-forming technique for smart antenna system," *International Journal of Computer Applications (0975–8887)*, Vol. 178, No. 11, 2019.
6. Mr, K. M., A. V. R. Holla, and H. M. Guruprasad, "Simulation of reduced complexity beamforming algorithms for mobile communication," *International Journal of Innovative Technology and Exploring Engineering (IJITEE)*, Vol. 1, No. 2, 2012.
7. Waghmare, P., P. Gupta, K. Gehlod, A. Shakya, and L. Malviya, "2×2 wideband array MIMO antenna for 5G spectral band," *2019 IEEE 5th International Conference for Convergence in Technology (I2CT)*, Bombay, India, 2019.
8. Chu, S., M. N. Hasan, J. Yan, and C. C. Chu, "Tri-band 2×2 5G MIMO antenna array," *2018 Asia-Pacific Microwave Conference (APMC)*, 2018.
9. Yashchyshyn, Y., et al., "28 GHz switched-beam antenna based on S-PIN diodes for 5G mobile communications," *IEEE Antennas and Wireless Propagation Letters*, Vol. 17, No. 2, 2018.
10. Abbas, E. A., M. Ikram, and A. Abbosh, "Dual functional MIMO antenna system for mmWave 5G and 2 GHz 4G communications," *IEEE International Symposium on Antennas and Propagation*, Atlanta, July 7–12, 2019.
11. Khalid, M., et al., "4-port MIMO antenna with defected ground structure for 5G millimeter wave applications," *Electronics*, Vol. 9, No. 71, 2020.
12. I. NTT DOCOMO, "5G Evolution and 6G," ed.: NTT DOCOMO, INC., 2020.
13. Rappaport, T. S., et al., "Wireless communications and applications above 100 GHz: Opportunities and challenges for 6G and beyond," *IEEE Access*, Vol. 7, 78729–78757, 2019.
14. Rappaport, T. S., Y. Xing, J. George, R. MacCartney, A. F. Molisch, E. Mellios, and J. Zhang, "Overview of millimeter wave communications for fifth-Generation (5G) wireless networks — With a focus on propagation models," *IEEE Transactions on Antennas and Propagation*, Vol. 65, No. 12, 18, 2017.
15. Singkang, L. M., K. A. H. Ping, H. Kunsei, K. Senthilkumar, K. Pirapaharan, A. M. A. Haidar, and P. R. P. Hoole, "Model based-testing of spatial and time domain artificial intelligence smart antenna for ultra-high frequency electric discharge detection in digital power substations," *Progress In Electromagnetics Research M*, Vol. 99, 91–101, 2021.
16. Singkang, L. M. B., K. A. H. Ping, and P. R. P. Hoole, "Electric discharges localization for substation fault monitoring using two elements sensor," *Journal of Computational and Theoretical Nanoscience*, Vol. 17, No. 2–3, 1009–1013, 2020.
17. Neiman, M. S., "The principle of reciprocity in antenna theory," *Proceedings of the IRE*, Vol. 31, No. 12, 666–671, 1943.
18. Hamdy, M. N., *An Introduction to LTE Smart Base Station Antennas*, M. N. Engineering (ed.), 2017.
19. Hoole, P. R., *Smart Antennas and Electromagnetic Signal Processing in Advanced Wireless Technology: with Artificial Intelligence Application and Coding*, River Publisher, USA-Denmark, 2020.
20. Pirapaharan, K., H. Kunsei, K. S. Senthilkumar, P. R. P. Hoole, and S. R. H. Hoole, "A single beam smart antenna for wireless communication in highly reflective and narrow environment,"

International Symposium on Fundamentals of Engineering, 2017.

21. Pirapaharan, K., H. Kunsei, K. S. Senthilkumar, P. R. P. Hoole, and S. R. H. Hoole, "A robust, 3-element triangular, reflector-less, single beam adaptive array antenna for cognitive radio network: Inter-element distance dependent beam," *Journal of Telecommunication, Electronic and Computer Engineering*, Vol. 8, No. 12, 4, 2016.
22. Zhang, J., S. Zhang, X. Lin, Y. Fan, and G. F. Pedersen, "3D radiation pattern reconfigurable phased array for transmission angle sensing in 5G mobile communication," *Sensor*, Vol. 18, No. 4204, 2018.
23. You, X., C. Zhang, X. Tan, S. Jin, and H. Wu, "AI for 5G: Research directions and paradigms," *SCIENCE CHINA Information Sciences*, Vol. 62, 2018.
24. Senthilkumar, K. S., et al., "A review of a single neuron weight optimization model for adaptive beam forming," *Journal of Telecommunication, Electronic and Computer Engineering (JTEC)*, Vol. 9, No. 3–10, 2017.